SPECIAL FEATURE

Password Protected
Circuit Breaker
System using Arduino

SiliconTech

The Science & Technology Magazine

# Digital Digest

Vol. 24 • Sep-Nov 2020

Our Vision: “To become a center of excellence in the fields of technical education & research and create responsible citizens”

# Cognitive Computing

Cognitive computing is based on simulation of the human thought process. It uses an amalgamation of different techniques like artificial intelligence, neural networks, machine learning, natural language processing, sentiment analysis and contextual awareness to find a solution to day-to-day problems just like humans. Cognitive computing redefines the class of problems that a computer can solve.

Computing has evolved a lot since its inception. The first era of computing started with Charles Babbage who introduced the concepts of programmable computer, navigational calculation and invented the mechanical computer. The second era experienced digitally programmable computers and different programming languages. The third era consists of cognitive computing techniques capable of imitating human behavior and reasoning to solve complex problems. There is a subtle difference in the approach of solving problems using AI and cognitive computing. AI tries to solve problems by finding patterns in the data space. It tries to draw conclusions based on these discovered patterns and makes decisions. Cognitive systems don't make decisions, rather they only supplement decision making. They try to simulate the human thought process to find solutions to complex problems. Cognitive systems provide information for humans to take decisions. Cognitive computing is a subset of artificial intelligence.

Cognitive systems are adaptive, dynamic in data gathering, understanding goals, and requirements. These systems are highly interactive and are able to communicate with humans in natural language. Several chatbots have already achieved this ability of communicating with consumers without human intervention. These systems remember previous interactions and provide information that is applicable at that moment. They are capable of identifying and comprehending contextual syntax, domain, regulations, user's profile, and objective. Some of these cognitive computing systems use both structured and unstructured data along with sensory inputs like visual, gestural, auditory etc. The unstructured data doesn't have a predefined data model as is the case with structured data.

There are several applications of cognitive computing. Vantage software is one such product that helps investment bankers to analyze huge data and provide suggestions as to where the clients' funds could be invested. LifeLearn provides a veterinary decision-support tool named Sofie which gives recommendations instantly, enabling busy vets to save time and look after patients with quality consideration. Malware attacks are prevented by using big data and machine learning algorithms. Cognitive Engine has the ability to multiply the value of all the IT investments by a combination of all the data and the processes of an organization, by cognitive intelligence, and suggest steps that hold the highest revenue impact on the company. Cogito is a multilingual cognitive software that provides humans the ability to evaluate and comprehend conversations in different languages. Its core algorithms are based on natural language processing.

Cognitive computing provides and improves the computer interaction that impersonates the working of the human brain and thereby helps in better decision-making processes.It provides customized results and deep insights by analysing vast data from different sources. Cognitive computing is an extremely powerful tool which is capable of providing us with excellent solutions and further extending the horizons of computation.

**Dr. Pamela Chaudhury**
*Dept. of CSE*

# Detecting Diabetic Retinopathy using Deep Learning

***Abstract :*** *Diabetic Retinopathy is one of the major causes of blindness around the world. This disease affects those people who suffer from diabetes and mainly aged diabetes patients. Many hospitals around the world try their best to conduct research and prevent blindness caused due to diabetic retinopathy. Being able to detect diabetic retinopathy before it is too advanced is a major challenge. This work focuses on detecting whether a patient has reached the stage of diabetic retinopathy or not and if yes, then which stage. The deep learning neural network is used to for this purpose classify the images of eyes of patients.*

**Keywords:** Deep learning, neural networks, image classification, medical imaging, diabetic retinopathy, medical imaging analysis, machine learning.

## I. INTRODUCTION

Diabetic retinopathy is the most common form of diabetic eye disease. Diabetic retinopathy usually only affects people who have had diabetes (diagnosed or undiagnosed) for a significant number of years [1]. Retinopathy can affect all diabetics and becomes particularly dangerous, increasing the risk of blindness, if it is left untreated. The risk of developing diabetic retinopathy is known to increase with age as well as with less well controlled blood sugar and blood pressure level. According to the NHS, 1280 new cases of blindness caused by diabetic retinopathy are reported each year in England alone, while a further 4,200 people in the country are thought to be at risk of retinopathy-related vision loss [2].

Diabetic retinopathy occurs when changes in blood glucose levels change the retinal blood vessels. In some cases, these vessels will swell up (macular oedema) and leak fluid into the rear of the eye. Diabetic retinopathy can gradually become more serious and progress from background retinopathy to seriously affecting vision and can lead to blindness. Like many conditions of this nature, the early stages of diabetic retinopathy may occur without symptoms and without pain. An actual influence on the vision will not occur until the disease advances. Symptoms of retinopathy to look out for include: Sudden changes in vision / blurred vision, Eye floaters and spots, Double vision, Eye pain

As, diabetic retinopathy is a leading cause of blindness among working-age adults, early detection of this condition is critical for good prognosis. Many adults who are suffering from diabetes have a high probability of being diagnosed with diabetic retinopathy at some stage of their life. In general, diabetic retinopathy is curable if detected at the early stages. But if the patient is diagnosed at a very severe stage, then it may not be curable at all [3]. This work focuses on detecting whether a person suffering from diabetes has diabetic retinopathy or not. The power of deep neural networks from the field of deep learning is employed for this purpose. In specific, the CNN (Convolutional Neural Network) architecture is used.

A large set of retina images were taken using fundus photography under a variety of imaging conditions. Fundus photography involves photographing the rear of an eye; also known as the fundus [4]. Specialized fundus cameras consisting of an intricate microscope attached to a flash enabled camera are used in fundus photography. The main structures that can be visualized in a fundus photo are the central and peripheral retina, optic discand macula [5]. Fundus photography can be performed with colored filters, or with specialized dyes including fluorescein and indocyanine green. An example of how the images look like is given in fig.1

***Figure 1****. A retina image taken using fundus Photography*

The main objective of the work is to use different types of images, different learning algorithms, and different neural network architectures and compare which combination gives the best results for detection of diabetic retinopathy. Using the current traditional cures and remedies the medical system is taking much time than needed to know about Diabetic retinopathy. We proposed a system in which the model can be trained using deep neural network on varieties of retina images and then by validating on the images weget better results can be otained. This takes less time than the usual traditional detection methodologies.

## II. DATA COLLECTION

The data set is collected from the Kaggle website [6]. The dataset contains retina scan images taken using fundus photography under a variety of imaging conditions. The dataset contains 3,662 images for training 1,928 images for testing. The default images provided on the website are colored images. They are very high-resolution images some ranging to around 4k dimensionality.

The dataset has been divided into a train directory, test directory, train.csv file, and test.csv file. The data is divided into five classes based on the severity of diabetic retinopathy. The following are the five classes:

0- No DR

1- Mild

2- Moderate

3- Severe

4- Proliferative DR

The numbering is done based on increasing severity where 0 means no diabetic retinopathy and 4 means the highest stage, that is, proliferative diabetic retinopathy. In the dataset, 1,805 images with no diabetic retinopathy, 370 images with mild, 999 images with moderate, 193 images with severe and 295 images with proliferative diabetic retinopathy were present. The number of images consider per class ratio is shown in fig. 2.

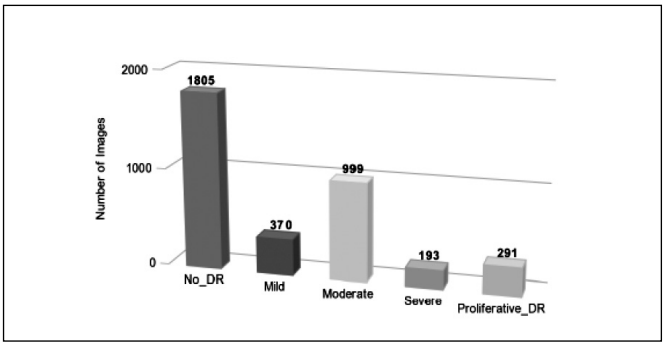


***Figure 2***. *Number of Images per Class*

Train directory contains all the images of retina that we train and validate the neural network model on. Train CSV file contains the labels corresponding to the images in the train directory. Similar is the structure for the test data as well. But the test CSV file does not contain the labels

## III. APPROACH

In this work, the severity of diabolic retinopathy is classified by the use of neural networks. The classification is done by ResNet34 [4]. This model as shown in fig 3contains 34 CNN layers. The first layer uses 7*7 filter and the next layers use 3*3. It uses Global average pooling layer and a 5-way fully-connected layer with Softmax in the end. ResNet34 solves the degradation problem i.e. the accuracy gets saturated and degrades rapidly on the increase in networkdepth.

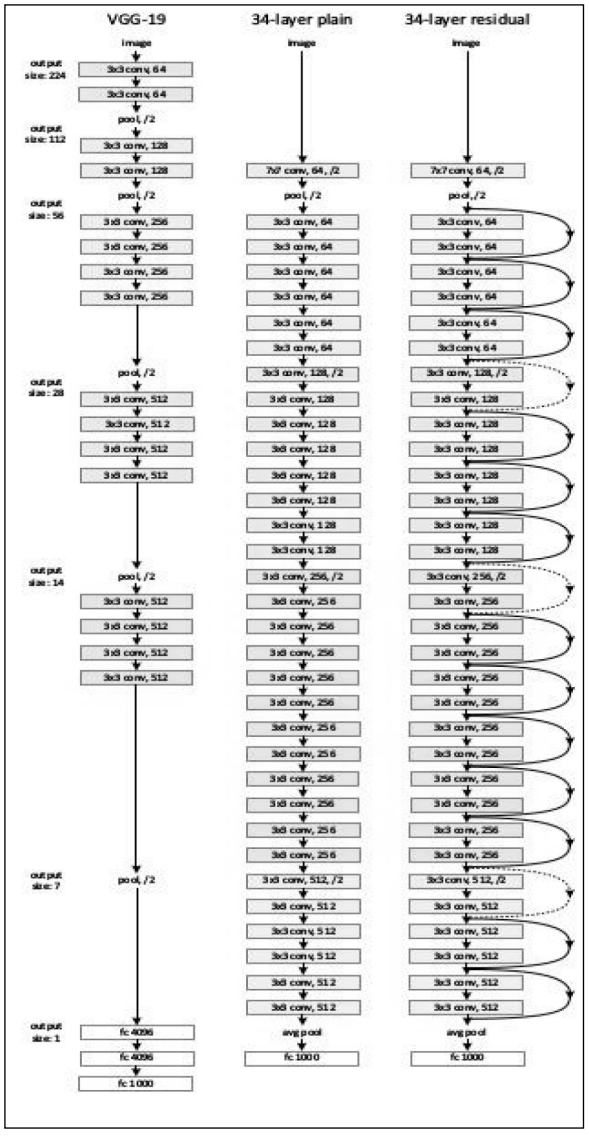


***Figure 3***. *ResNet34 blocks*

## IV. EXPERIMENTAL RESULTS

For the first stage of the experimentation the ResNet34 is trained for 20 epochs and for 3 epochs after finding the optimal learning rate of the neural network. This process is repeated for all the three different colored datasets (colored, grayscale, andgaussian).

### A. Colored Images Results

During the initial training of colored images, for the first 20 epochs the best error rate is 0.195355. After learning rate optimization the best error rate of 0.178962 is achieved. The lowest training loss is 0.441782 and validation loss is 0.541847 as shown in figure 4.

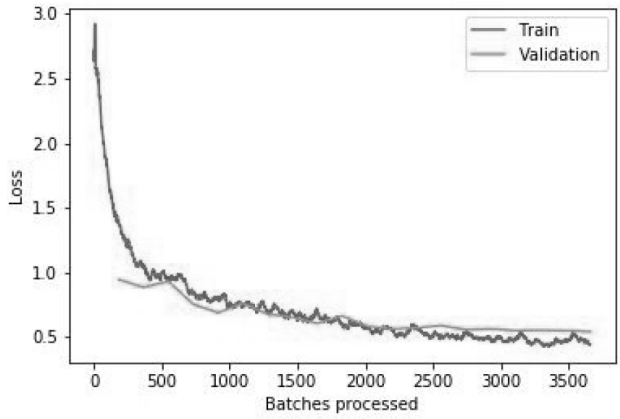


***Figure 4**. Colored Images Traning Loss after 20 Epochs*

### B. Grayscale Images Results

For grayscale images, the lowest error rate after 20 epochs of training is 0.196721 with best training loss of 0.480602 and best validation loss of 0.520497 as shown in figure 5.

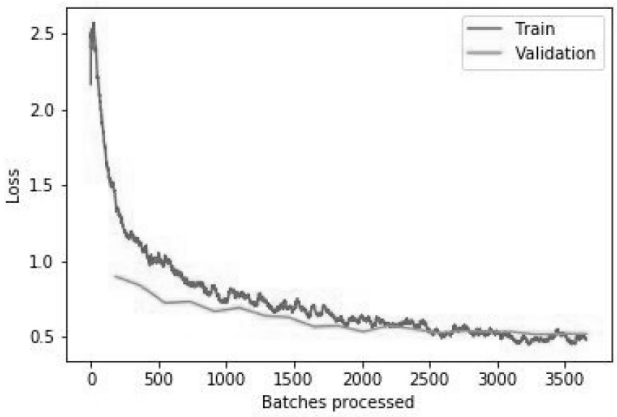


***Figure 5**. Grayscale Images Training Loss After 20 Epochs*

### C. Gaussian Filtered Images Results

For grayscale images, the lowest error rate after 20 epochs of training is 0.221311 with best training loss of 0.478799 and best validation loss of 0.578836 as shown in figure 6.

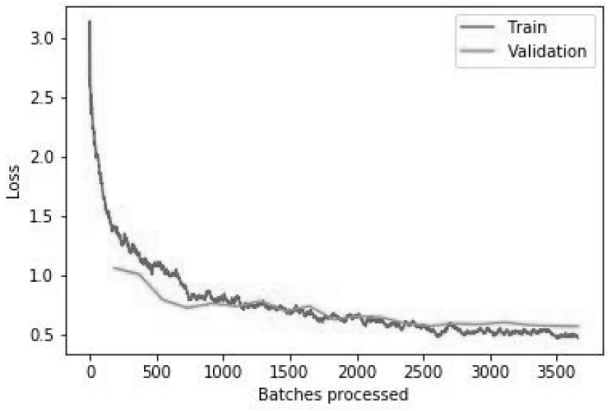


***Figure 6**. Gaussian Filtered Images Training Loss After 20 Epochs*

### D. Training Result Tables

The following tables show the results of training on colored, grayscale, and gaussian filtered retina images. We have trained each of the image sets for 20 epochs. In the following tables 1,2 and 3the results of the last three epochs are shown

| epoch | train_loss | valid_loss | error_rate |
|---|---|---|---|
| 18 | 0.456303 | 0.551894 | 0.207650 |
| 19 | 0.483539 | 0.548007 | 0.214481 |
| 20 | 0.441782 | 0.541847 | 0.211749 |

***Table 1**. Last three epoch results for colored retina images*

| epoch | train_loss | valid_loss | error_rate |
|---|---|---|---|
| 18 | 0.492623 | 0.516096 | 0.200820 |
| 19 | 0.512907 | 0.520497 | 0.200820 |
| 20 | 0.480602 | 0.521209 | 0.196721 |

***Table 2**. Last three epoch results for grayscale retina images*

| epoch | train_loss | valid_loss | error_rate |
|---|---|---|---|
| 17 | 0.519309 | 0.587234 | 0.229508 |
| 18 | 0.510745 | 0.579334 | 0.224044 |
| 19 | 0.478799 | 0.578836 | 0.221311 |

***Table 3**. Last three epoch results for Gaussian filtered retina images*

From the above tables, it can be observed that the training loss after 20 epochs is the least for colored retina images (Table 1). For the error rate, the least error rate in the case of training grayscale images is obtained. But the training loss is more in case of grayscale images than in colored images. The neural network seems to be performing the worst in the case of gaussian filtered images when taking the error rate as a result metric. Also, the validation loss is the highest in this case. The results show that perhaps, training a bigger neural network model on a mixture of all images may provide much better results.

### E. Validation Results

The validation results provide a good insight of how good/bad the neural network model is performing while validating on the dataset. Figures 7, 8, and 9 shows the confusion matrix interpolation plot for the validation of the retina images. The figures correspond to colored images validation, grayscale images validation, and gaussian filtered images validation results respectively.It may be clearly observe that in all cases, the ResNet34 neural network model is perfectly classifying the No_DRclass. This is because, this class has the most number of images (almost 1800 images) and it is getting enough images for that class to learn the patterns. Whereas, for the other classes, the number images are quite less, and below 1000 images per class as well.

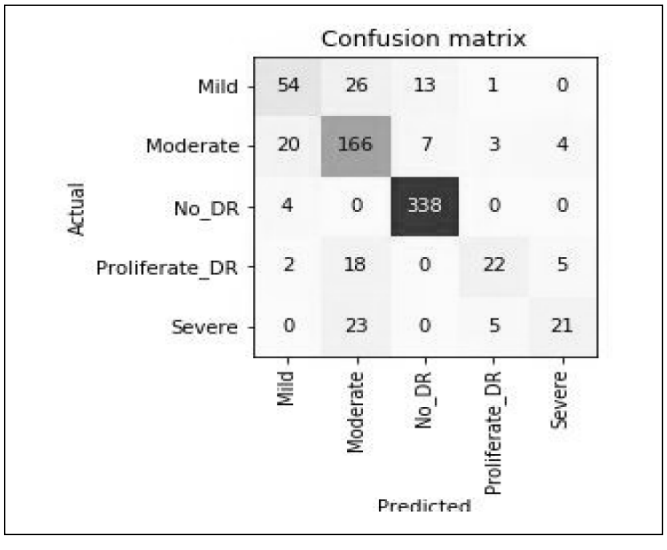


***Figure 7**. Confusion Matrix for Colored Images Validation*

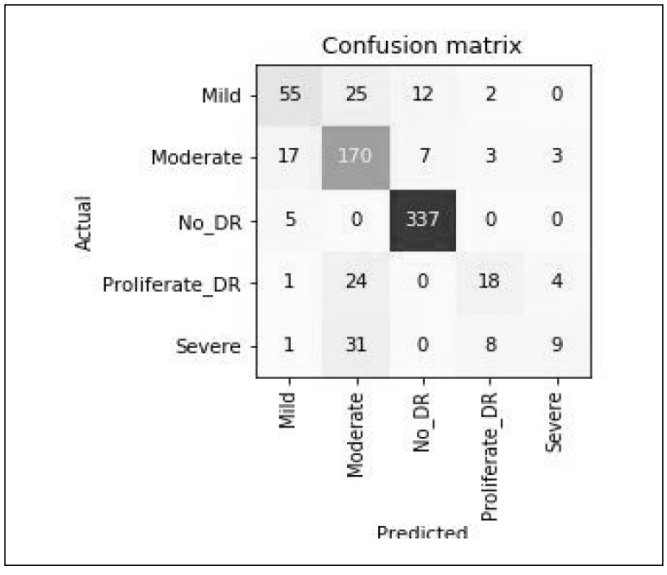


***Figure 8**. Confusion Matrix for Grayscale Images Validation*

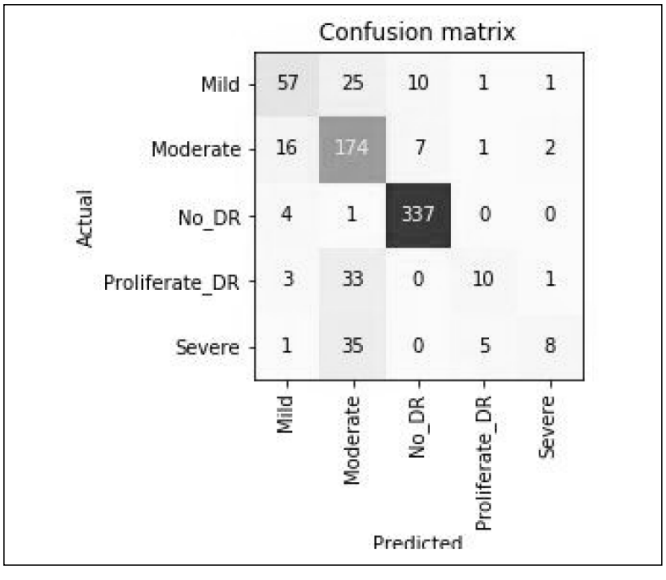


***Figure 9**. Confusion Matrix for Gaussian Filtered Images Validation*

The validation mistakes in some cases are quite profound as well. For example, in the case of colored retina images validation, the neural network model is classifying 18 Moderate class as Proliferate_ DRclass. And in total, it is misclassifying 131 images out of 732 validation images. In the case of grayscale validation images, the neural network model is misclassifying 143 images out of 732 validation images.Here, validation results are worse than the colored images validation results. In the case of gaussian filtered validation images, the neural network model is misclassifying 146 images out of 732 validation images. The validation results

are the worst here. Mostly because, after applying gaussian filtering to the retina images, they are losing many of the pixel and color features. Therefore, the neural network model is finding it difficult to learn all the important features.

### F. Results from the Larger Dataset

This dataset contains 35,126 images and is 35 gigabytes in size. For this specific dataset, we trained two different neural networkmodels: ResNet34, ResNet50. We are showing the best set of results that were obtained by training the ResNet50 model. The SGD optimizer is used with image augmentation and learning rate scheduler for hyperparameter tuning.

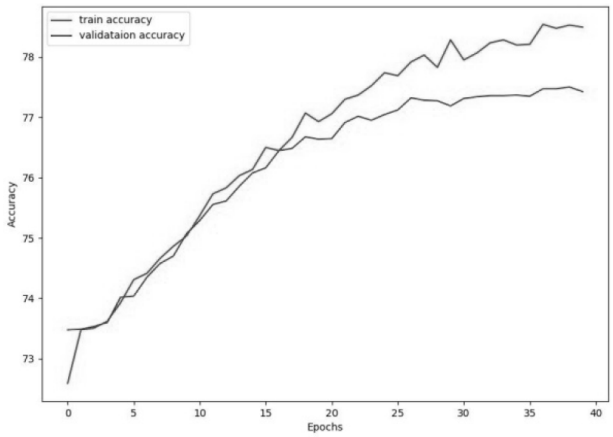


***Figure 10**. Accuracy plot for ResNet50 trained for 40 epochs with SGD optimizer and with data augmentation*

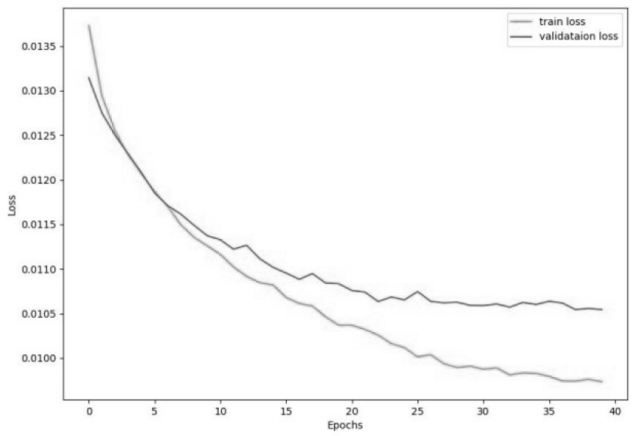


***Figure 11**. Loss plot for ResNet50 trained for 40 epochs with SGD optimizer and with data augmentation*

## V. CONCLUSIONS:

The presented methods using deep learning and neural networks on the retina images achieves 78% validation accuracy. This is 3% higher than manual method of detection. Although the increase in accuracy is not too much but it can be further improved using larger neural networks for training and using more robust image processing techniques. Also, using larger images for training the neural network may help capture and extract more useful features.

**ACKNOWLEDGMENT**

We express our sincere gratitude to our project guideDr. Ramakrushna Swain of CSE department for his guidance in carrying out this projectwork.

## VI. REFERENCES:

[1] Goodfellow et al., “Convolutional Networks”, in Deep Learning, pp. 326 - 366.

[2] Panwar et al., “Fundus Photography in the 21st Century—A Review of Recent Technological Advances and Their Implications for Worldwide Healthcare”. Telemedicine and e-Health, March 2016.

[3] Mingyuan Xin and Yong Wang. “Research on image classification model based on deep convolution neural network”.EURASIP Journal on Image Processing.

[4] JaakkoSahlsten, Joel Jaskari, JyriKivinen, Lauri Turunen, Esajanio, KustaaHietala, Kimmo Kaski, “Deep Learning Fundus Image Analysis for Diabetic Retinopathy and Macular Edema Grading,” in Science Reports, 2019.

[5] Dilip Singh Sisodia, Shruti Nair, Pooja Khobragade. “Diabetic Retinal Fundus Images: Preprocessing and Feature Extraction For Early Detection of Diabetic Retinopathy”. Biomedical and Pharmacology Journal.

[6] “Kaggle Diabetic Retinopathy Detection,” 2015. [Online]. Available: https://www.kaggle. com/c/diabetic-retinopathy-detection.

**Harshit Verma, Rashmiranjan Pradhan, Sovit Ranjan Rath, Jogesh Agrawal**

*8th Sem. IT*

# Automation and Monitoring for the Military

***Abstract :*** *: This project can be used by the military force to seek help during any war or sudden attack. So, this project aims to improve the communication and provide back-up for them. The basic idea behind this project is to keep a count on the pulse rate of the force men and the location of all the troops and if any disturbance, a signal and with the location would be send to the control unit and even to the other troops to be alert and provide back up and aids to them with the help of IOT techniques, RF module and GSM technology.*
*Keywords: Internet of things (IOT),Global System for Mobile Communications (GSM), radio frequency (RF),defence readiness condition (DEFCON), Valid Transmission (VT), Global Positioning System (GPS)*

**Keywords:** Internet of things (IOT),Global System for Mobile Communications (GSM), radio frequency (RF),defence readiness condition (DEFCON), Valid Transmission (VT), Global Positioning System (GPS)

## I. INTRODUCTION

In past centuries communicating a message usually required someone to go to the destination, bringing the message. Drums, horns, flags, and riders on horseback were some of the early methods the military used to send messages over distances.Then came the era of Electric telegraph by Samuel F.B. Morse. In his successful demonstration of electric communication. Then in 19th century the military used handheld trans-receiver. As there are many technology development seen in every field so there should be some development in the military field also so there can be better communication within the soldier troops and the main station. In the all past attacks we saw that due to lack in communication within our soldiers we lost many of our great assets This technology that we are developing could help us in doing the same [1].

Drums, horns, flags, and riders on horseback were some of the early methods the military used to send messages over distances. In the middle 20th century radio equipment came to dominate the field. Many modern pieces of military communications equipment are built to both encrypt and decode transmissions and survive rough treatment in hostile climates [2]. They use different frequencies to send signals to other radios and to satellites. Military communications - are activities, equipment, techniques, and tactics used by the military in some of the most hostile areas of the earth and in challenging environments such as battlefields, on land, underwater and also in air. Military communications include command, control and communications and intelligence and were known as the C3I model before computers were fully integrated [3]. The U.S. Army expanded the model to C4I when it recognized the vital role played by automated computer equipment to send and receive large, bulky amounts of data. The advent of distinctive signals led to the formation of the signal corps; a group specialized in the tactics of military communications. The signal corps evolved into a distinctive occupation where the signaller became a highly technical job dealing with all available communications methods including civil ones. In the modern world, most nations attempt to minimize the risk of war caused by miscommunication or inadequate communication. As a result, military communication is intense and complicated, and often motivates the development of advanced technology for remote systems such as satellites and aircraft, both manned and unmanned, as well as computers. Computers and their varied applications have revolutionized military communications. Although military communication is designed for warfare, it also supports intelligence-gathering and communication between adversaries, and thus sometimes prevents war.

There are six categories of military communications: the alert measurement systems, cryptography, military radio systems, nuclear command control, the signal corps, and network-centric warfare [4]. The alert measurement systems are various states of alertness or readiness for the armed forces used around the world during a state of war, act of terrorism or a military attack against a state. They are known by different acronyms, such as DEFCON, or defence readiness condition, used by the U.S. Armed Forces. Cryptography is the study of methods of converting messages to a form unreadable except to one who knows how to decrypt them [5,6]. This ancient military communications art gained new importance with the rise of radio systems whose signals travelled far and were easily intercepted. Cryptographic software is also widely used in civilian commerce.

The whole project that is done can be divided into mainly 2 parts: Main and Base station

**1. Main station :**

Fig. 1 shows the main station.

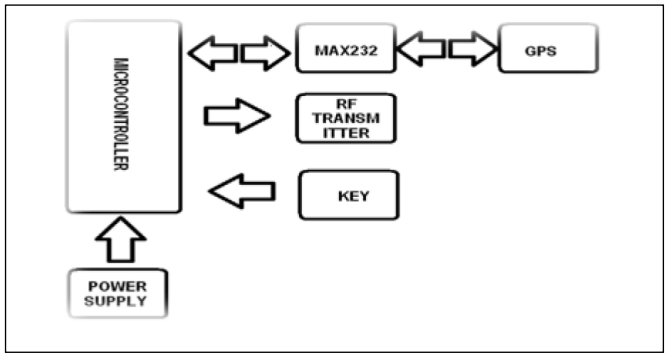


***Fig. 1** shows the main station.*

**2. Base station:**

Fig. 2 shows the base station

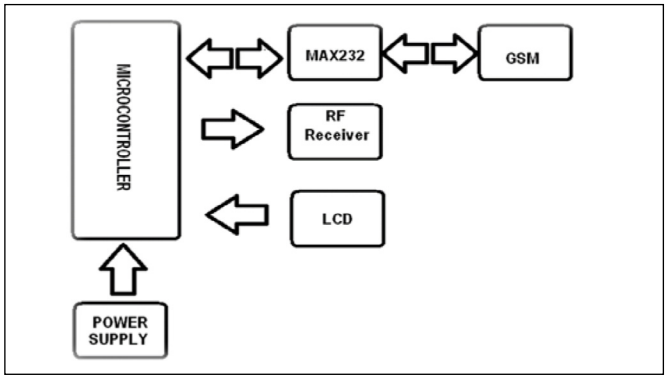


***Fig. 2** Base station*

## II. POWER SUPPLY

The microcontroller and other devices get power supply from AC to Dc adapter through 7805, 5 volts regulator. The adapter output voltage will be 12V DC non-regulated [7]. The 7805/7812 voltage regulators are used to convert 12 V to 5V/12V DC. Fig. 3 shows the power supply circuit.

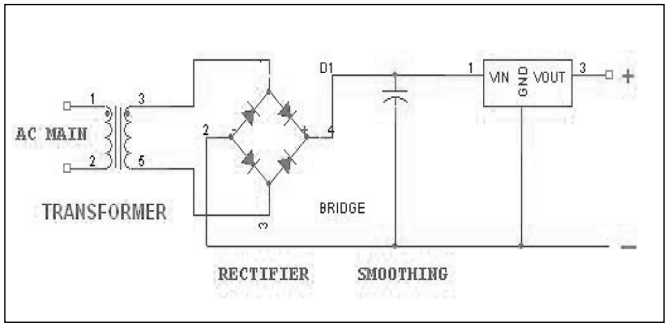


***Fig. 3** Power Supply Circuit*

**A. Regulated Power Supply**

A power supply containing means of maintaining essentially constant output voltage or output current under changing load conditions.

**B. Bridge Rectifier**

A bridge rectifier can be made using four individual diodes, but it is also available in special packages containing the four diodes required. It is called a full wave rectifier because it uses the entire AC wave (both positive and negative section). 1.4 volt is used up in the bridge rectifier because each diode uses 0.7 volt when conducting and there are always two diode conducting. The maximum current they can pass rates bridge rectifiers and the maximum reverse voltage they can withstand (this must be at least three times the supply RMS voltage so the rectifier can withstand the peak voltages.

**C. Smoothing**

Smoothing is performed by a large value electrolyte capacitor connected across the DC supply to act as a reservoir, supplying current to the output when the varying dc voltage from the rectifier is falling. The diagram shows the unsmoothed varying dc and the smoothed DC [8,9]. The capacitor charges quickly near the peak of the varying DC, and then discharges as it supplies current to the output.

**D. Regulator**

Voltage regulator IC shown in fig. 4 available with fixed (typically 5, 12, and 15 volts) or variable output voltages. The maximum current they can pass also rates them. Negative voltage regulators are available, mainly for use in dual supplies. Most regulators include some automatic protection from excessive current and overheating.

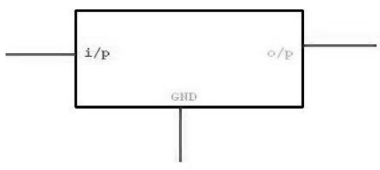


***Fig. 4** Regulator*

## III.MICRO-CONTROLLER

The AT89C51 is a low-power, high-performance CMOS 8-bit microcontroller with 8K bytes of in-system programmable Flash memory. The device is manufactured using Atmel's high-density non-volatile memory technology and is compatible with the industry-standard 80C51 instruction set and pin out. The on-chip Flash allows the program memory to be reprogrammed in-system or by a conventional non-volatile memory

programmer. By combining a versatile 8-bit CPU with in-system programmable Flash on a monolithic chip, the Atmel AT89S52 is a powerful microcontroller which provides a highly-flexible and cost-effective solution to many embedded control applications. The AT89S52 provides the following standard features: 8K bytes of Flash, 256 bytes of RAM, 32 I/O lines, Watchdog timer, two data pointers, three 16-bit timer/counters, a six-vector two-level interrupt architecture, a full duplex serial port, on-chip oscillator, and clock circuitry [10].

## IV. RADIO FREQUENCY RECEIVER AND TRANSMITTER MODULE

### A. Decoder

HT12D shown in Fig. 5, is a decoder at standby mode initially i.e, oscillator is disabled and a HIGH on DIN pin activates the oscillator. Thus the oscillator will be active when the decoder receives data transmitted by an encoder. The device starts decoding the input address and data. The decoder matches the received address three times continuously with the local address given to pin A0 – A7. If all matches, data bits are decoded and output pins D8 – D11 are activated. This valid data is indicated by making the pin VT (Valid Transmission) HIGH. This will continue till the address code becomes incorrect or no signal is received.

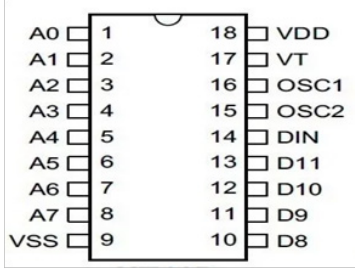


***Fig. 5*** *HT12D*

### B. Encoder:

Fig. 6 shows HT12E a 212 series encoder IC (Integrated Circuit) for remote control applications. It is commonly used for radio frequency (RF) applications. By using the paired HT12E encoder and HT12D decoder we can easily transmit and receive 12 bits of parallel data serially. HT12E simply converts 12bit parallel data in to serial output which can be transmitted through a RF transmitter. These 12bit parallel data is divided in to 8 address bits and 4 data bits. By using these address pins we can provide 8 bit security code for data transmission and multiple receivers may be addressed using the same transmitter.

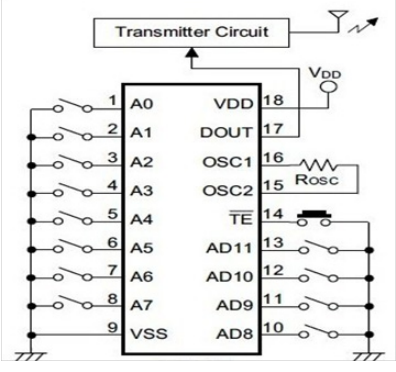


***Fig. 6*** *HT12E*

The proposed model was run using MATLAB/ SIMULINK.Comparison between the performances of the proposed system and the conventional system is carried out in terms of power generated using the PV units.When the irradiation values are changed to simulate partial shading scenario; the power produced by the conventional converter is reduced drastically. Whereas, in power supplied by the proposed system is comparatively more.

When the irradiation of a single unit is set to 600 W/sq.m from 650 W/sq.m, the total power generated from all the four PV units is around 600 W for the proposed system while it is only 400 W for the conventional system. Such small variations are very frequent in normal operation hence it can amount to considerable difference in the energy extracted. For further larger difference in insolation, the results are more and more promising with the proposed method.

The proposed method involving MISO converter does not require bypass diodes across individual PV units.

## V. ADDITIONAL DEVICES

### A.GSM

Designed for global market, SIM900 is a Tri-band GSM/GPRS engine that works on frequencies EGSM 900 MHz, DCS 1800 MHz and PCS1900 MHz SIM300 provides GPRS multi-slot class 10 capability and support the GPRS coding schemes CS-1, CS-2, CS-3 and CS-4.

With a tiny configuration of 40mm x 33mm x 2.85 mm, SIM300 can fit almost all the space requirement in your application, such as Smart phone, PDA phone and other mobile device. The GSM 07.05 commands are for performing SMS and CBS related operations. SIM300 II supports both Text and PDU modes.

### B.GPS

The Global Positioning System (GPS) is a U.S.-owned utility that provides users with positioning, navigation, and timing (PNT) services. This system consists of three segments: the space segment, the control segment, and the user segment. The U.S. Air Force develops, maintains, and operates the space and control segments. GPS is a system. It's made up of three parts: satellites, ground stations, and receivers.Satellites act like the stars in constellations—we know where they are supposed to be at any given time.The ground stations use radar to make sure they are actually where we think they are.A receiver, like you might find in your phone or in your parents car, is constantly listening for a signal from these satellites. The receiver figures out how far away they are from some of them.

### C. Heart Rate

Pulse Sensor is a low cost, very small size a plug-and-play heart rate sensor for MCU boards. It can be used by students, artists, athletes, makers, and game & mobile developers who want to easily incorporate live heart-rate data into their projects. Fig. 7 shows a heartbeat sensor. Pulse Sensor Amped adds amplification and noise cancellation circuitry to the hardware. It's noticeably faster and easier to get reliable pulse readings. Pulse Sensor works with either a 3V or 5V MCU.

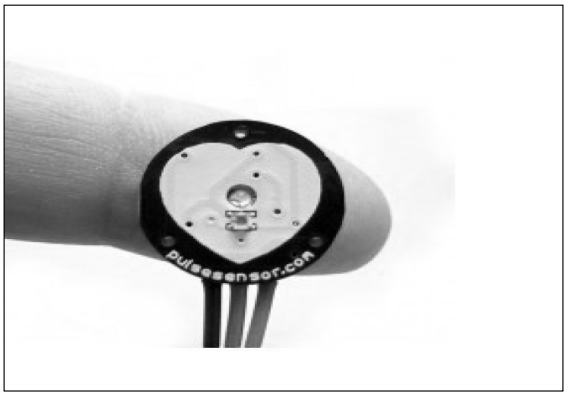


***Fig. 7*** *Heart beat sensor*

A Color-Coded Cable, with a standard male header connectors. Plug it straight into an MCU or a Breadboard. No soldering is required. An Ear Clip, perfectly sized to the sensor. It can be hot-glued or epoxied to the back of the sensor to get reading from an ear lobe [11].

## VII. PROCEDURE

The AC supply was given to the power supply circuit where it was stepped down to 0-18 v. Further the voltage was converted to DC by passing through bridge rectifier. The output of the bridge rectifier was pulsating DC, so to convert it to pure DC an electrolyte capacitor was used. This current is then passed through 7805 and 7812 voltage dividers to get 5v and 12v respectively. The supply was given to the micro controller circuit to turn it on. This microcontroller gets clock pulse through crystal oscillator. The microcontroller gets the output from the sensor and the GPS. This send the result to the RFID transmitter. The RFID receives the information decodes the analog signal and send this to the microcontroller. The information is displayed in the LCD. All these information's are send to the headquarters through SIM900 in form of text message.

## VIII. HARDWARE RESULTS

Fig. 8 and 9 shows the hardware results.

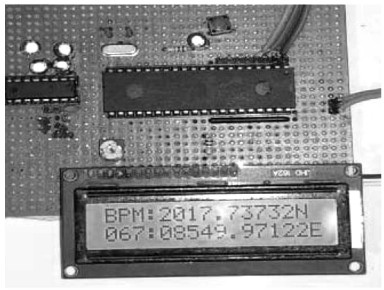


***Fig. 8*** *Hardware Result*


***Fig. 9*** *Hardware results*

## IX. CONCLUSIONS

The rate of death of soldiers in India in last 5 years rose to 93% death of security personnel in terror attacks. By implementing this project we would at least decrease this rate or save some by providing immediate help

## REFERENCES

1. https://www.engineersgarage.com/electronic-components/rf-module-transmitter-receiver
2. http://ww1.microchip.com/downloads/en/devicedoc/doc1919.pdf
3. https://en.wikipedia.org/wiki/AN/PRC-148
4. en.wikipedia.org
5. http://www.ti.com/lit/ds/symlink/max232.pdf
6. https://www.electrical4u.com/crystal-oscillator/
7. https://www.tutorialspoint.com/sinusoidal_oscillators/sinusoidal_crystal_oscillators.htm
8. https://components101.com/ics/lm339-pinout-features-datasheet
9. http://www.circuitstoday.com/8051-microcontroller
10. https://www.circuitspedia.com/regulated-dc-power-supply-230v-ac-to-12v-dc-and-5v-dc/
11. http://www.circuitstoday.com/interfacing-lcd-to-arduino

**Abhishek A,Debashis Majhi,**
**Indrani Singh, Aurochit Mohanty,**
**Suvendu Kar, Lopamudra Rath**
*Dept. of EEE*

# Design of a Miniaturized Circular Microstrip Patch Antenna for 5G Applications

***Abstract :*** *In this paper, a novel proximity-coupled fed microstrip Circular Patch Antenna (CPA) is proposed for 5G applications. The proposed CPA resonates at a frequency of 3.5 GHz. The simulation of the proposed CPA is done using High Frequency Structure Simulator (HFSS) software. The parametric optimization feature available in HFSS Software is used for determining the optimized dimensions of the proposed CPA. The optimized compact CPA is having a substrate of length 30 mm, and width 45 mm. The radius of the radiating patch is 13.005 mm. The proposed antenna is having an excellent S11 characteristic and impedance matching. The S11 is found to be -40.2827 dB. The CPA also has a substantial gain of 5.8 dB. The VSWR is nearly ideal (1.02) and the CPA has an efficiency of 88.40% and serves a bandwidth of 200 MHz. With such alluring features, the proposed CPA can be a suitable candidate for a variety of 5G applications such as the Internet of Things (IoT), Machine to Machine (M2M) Communication, etc.*

**Keywords:** —Circular patch antenna, 5G, HFSS, proximity-coupled feed, bandwidth, gain, efficiency, optimization

## I. INTRODUCTION

5G is one of the most recent technologies these days and moreover, everyone is curious about this technology. It has a number of benefits like seamless coverage, higher data rate, low latency, and high reliability. Moreover, the quality of video services is also expected to improve. As per a study done by the Telecom Regulatory Authority of India (TRAI) in [1], it has been found that the mobile data usage per month in India has increased from 39 petabytes in June 2016 to 4178 petabytes in September 2018. Moreover, the demand for higher data rates has increased for which it is expected that within a few years it is necessary to switch from the current generation to a higher generation, to a higher frequency band. 5G uses higher frequency ranges for its applications for which the microstrip patch antennas are the best candidates. Moreover, the microstrip patch antennas are economic, light-weight and easy to manufacture. As the frequency is increased, the size of the devices reduces. Therefore, the antennas can be expected to be compact and miniaturized so that they can be used in different hand-held devices.

The spectrum is the lifeline of any communication. These are of three different categories – low frequency, medium frequency, and high frequency. Based upon different requirements and applications, 5G communication technology uses the medium and high frequencies for the communication purpose for higher data rates and high system capacity in dense deployments. There are three pioneer bands for 5G technology, been targeted or allocated in India. These are – 700 MHz, 3.5 GHz and 26/28 GHz [1]. Out of these three pioneer bands, the proposed antenna in this paper resonates at 3.5 GHz.

Literature surveys were done on 5G antennas and different feeding techniques. The following are some of the observations:

In [2], the 5G antenna operates at 38 GHz and 54 GHz. The antenna has a high gain of 6.9 dB and 7.4 dB at 38 GHz and 54 GHz respectively. However, the S11 parameter is found to be -15.5 dB and -12 dB for 38 GHz and 54 GHz respectively. Moreover, the bandwidth at 38 GHz and 54 GHz is observed to be 1.94 GHz and 2.05 GHz respectively. The model also illustrated a 5G antenna array for different resonating frequencies at 38 GHz, 47.7 GHz, and 54 GHz with S11 parameter values -13.5 dB, -22.5 dB, and -18 dB respectively.

A comparison among different techniques for feeding for simple rectangular, circular and triangular patch antenna for a frequency of 2.45 GHz is made in [3]. It is observed that when the shape of the patch is changed, there is no such significant change in parameters like gain, directivity, and efficiency. However, when the different types of feeding techniques were applied on the patch, it is observed that by using proximity coupled feeding technique, the directivity remained almost the same but the gain and efficiency increased.

In [4], a compact and miniaturized rectangular patch antenna (RPA) is proposed. It resonates at a frequency of 10.5 GHz with the S11 parameter value as -18.27 dB, a gain of 4.46 dB and a bandwidth of 380 MHz. It has an acceptable VSWR value of 2.13 dB, which is suitable for wireless applications.

An RPA resonating at 3.5 GHz frequency is proposed for 5G applications [5]. The antenna is a miniaturized one with a dimension of 30 mm × 45 mm. It has a maximum gain of 7 dB. However, the S11 parameter is observed to

be -20.38 dB. The bandwidth, in this case, is found to be 100 MHz.

The substrate plays a vital role in the case of proximity-coupled feeding technique. In [6], it is observed that in this technique, if the substrate having higher relative permittivity is kept at the top and the substrate with lower relative permittivity is kept at the bottom, the gain will be higher.

## II. ANTENNA DESIGN PROCEDURE AND STRUCTURE

The CPA is the most accepted design next to a rectangular patch antenna. The antenna consists of a thin metallic circular strip on the top of a substrate.

The initial radius of the patch with Rogers RT/Duroid 5880 as the substrate is found using the following equation [7].

$$R = \frac{F}{\{1+\frac{2h}{\delta\varepsilon_r F}[\ln(\frac{\delta F}{2h})+1.7726\}^{1/2}}$$

Where $F = \frac{8.791\times 10^{9}}{f_r\sqrt{\varepsilon_r}}$

$R$ = Radius of the circular patch in cm.
$h$ = Height of the substrate in cm.
$\varepsilon r$ = Dielectric constant of the substrate.
$fr$ = Resonant frequency of the patch in Hz.

Later, the CPA is designed with two substrate layers using proximity coupled feeding technique. The dimensions of the CPA and the proximity feed are optimized using parametric optimization in-built in HFSS. The enhanced parameters of the CPA are as shown in Table I.

Table I. Dimension Of Circular Patch Antenna

| Dimension | Value (mm) |
|---|---|
| Length of ground plane/ substrate (L) | 45 |
| Width of ground plane/ substrate (W) | 30 |
| Radius of the patch (R) | 13.005 |
| Height of the bottom substrate (hb) | 1.5 |
| Height of the top substrate (ht) | 1.6 |
| Length of the proximity feed (Lf) | 26.49 |
| Width of the proximity feed (Wf) | 2.85 |

The different views of the proposed CPA are as shown in Fig. 1. The feeding of the microstrip patch antennas can be done in different ways. Some of them are microstrip line feed, coaxial probe feed, inset feed, aperture-coupled feed, proximity coupling, etc. [7]. The proposed antenna makes the use of the proximity-coupled feeding technique. This feeding technique has numerous advantages such as larger bandwidth and low spurious radiation

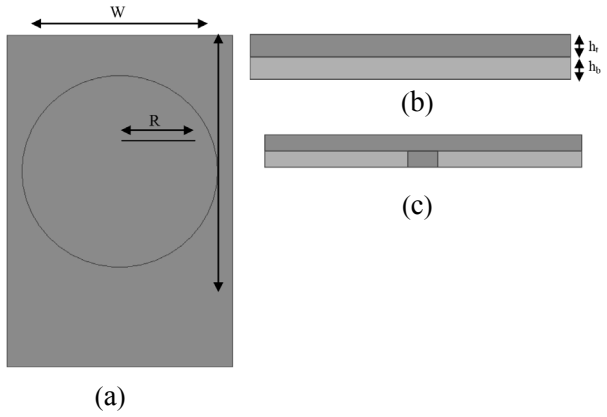


***Fig. 1****. CPA with Proximity-coupled feed (a) Top view (b) Side view (c) Front view*

The proximity-coupled feed line is given between the two substrates – FR4 Epoxy ($\varepsilon r$ = 4.4) and Rogers RT/ Duroid 5880 ($\varepsilon r$ = 2.2). In order to increase the gain, the FR4 Epoxy is used as the top substrate and Rogers RT/ Duroid 5880 substrate is used as the bottom substrate [6]. The proximity-coupled feed line is as shown in Fig. 2.

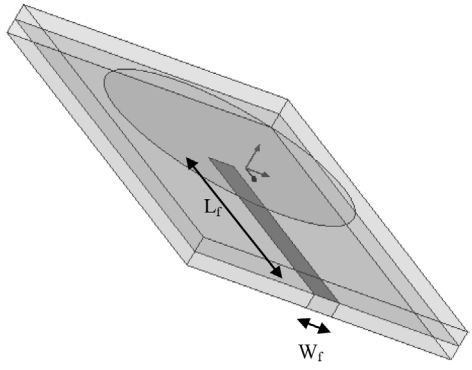


***Fig. 2*** *Proximity – coupled feed given between the two layers of substrates*

## III. RESULTS AND DISCUSSIONS

The design and the simulation of the proposed antenna are done via ANSYS HFSS software. It resonates at a frequency of 3.5 GHz. The CPA has an excellent S11 parameter with a value of –40.2827 dB. The bandwidth of the proposed CPA is 200 MHz. According to the TRAI [1], the bandwidth of 3.5 GHz 5G band extends from 3.3 GHz to 3.6 GHz. The proposed CPA, in this case, has a bandwidth of 200 MHz and it extends from 3.4 GHz to 3.6 GHz, which is suitable for the 5G band as mentioned. The S11 characteristic of the CPA is as shown in Fig. 3

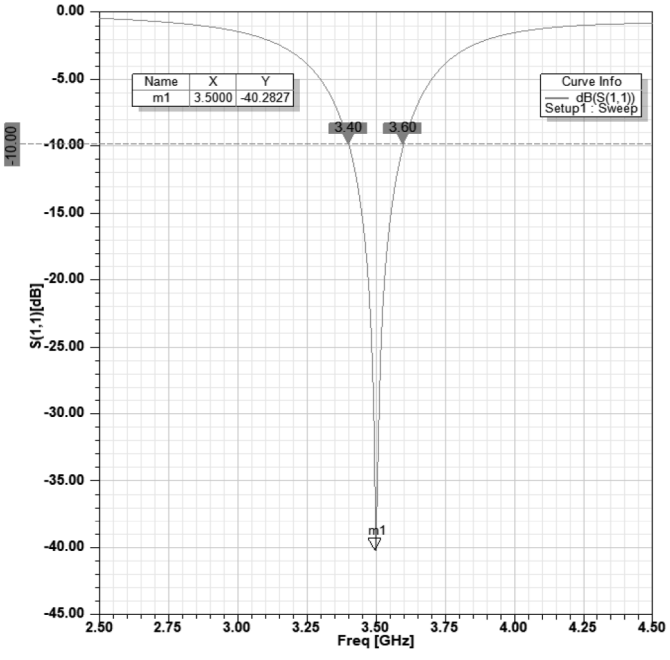


***Fig. 3*** *(dB) versus Frequency (GHz) of the proposed CPA resonating at 3.5 GHz*

For an antenna, the impedance must be matched properly in order to satisfy the maximum power transfer theorem [7]. The antenna is excited via a feed line having an impedance of 50 Ohm. According to the results, the proposed CPA has a real part of 50.99 Ohm and an imaginary part of 0.15 Ohm

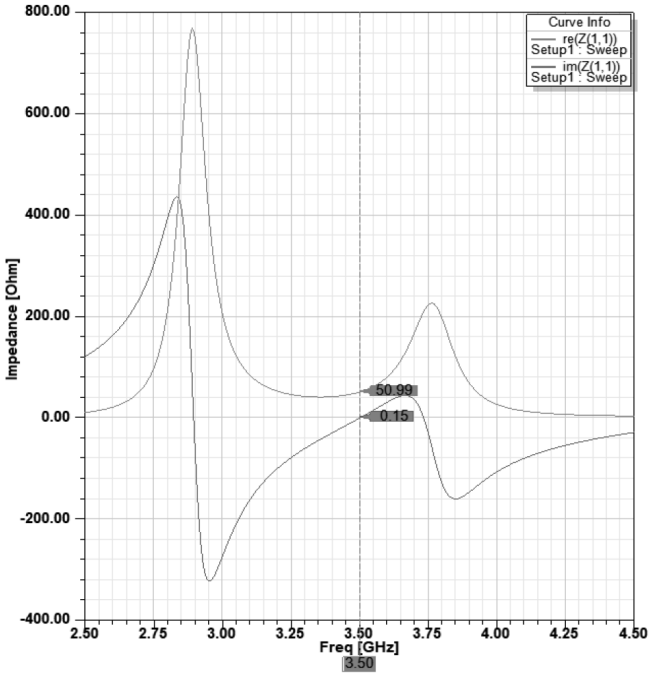


***Fig. 4*** *Impedance characteristics of the proposed CPA resonating at 3.5 GHz*

The CPA has an excellent impedance matching and therefore, maximum signal transmission can take place. The impedance characteristic of the proposed CPA is as shown in Fig. 4.

The radiation pattern of the proposed microstrip circular patch antenna is as shown in Fig. 5. The plot signifies that the radiation pattern is almost omnidirectional in nature.

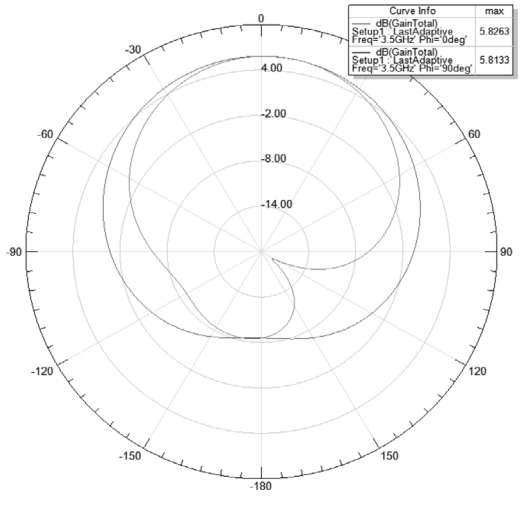


***Fig. 5.*** *Radiation Pattern of the proposed CPA resonating at 3.5 GHz*

The gain of the CPA in E-Plane is 5.8263 dB and that of the H-Plane is 5.8133 dB. The antenna is highly efficient with an efficiency of 88.40 %.

Ideally, the VSWR value should be 1 and in this case, the CPA has a VSWR value of 1.02, which is nearly ideal. So, the reflected power will be less than 1% and therefore, there will be a maximum transmission of the signals. The VSWR characteristic of the CPA is as shown in Fig. 6.

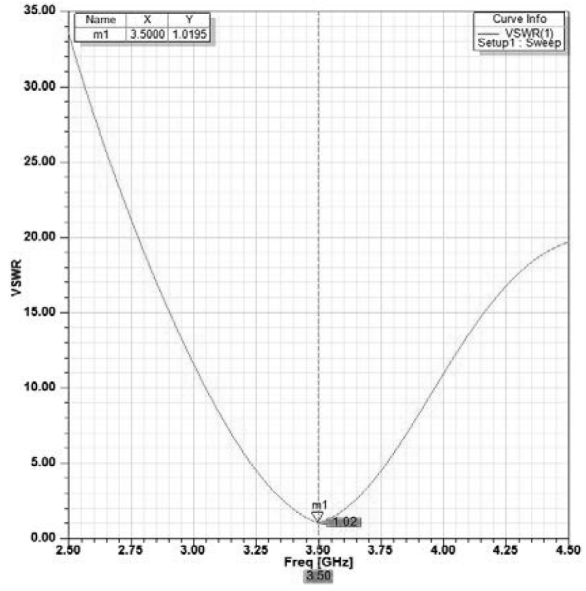


***Fig. 6.*** *VSWR characteristics of the proposed CPA*

In this paper, a CPA has been designed for 5G applications. The design and simulation are done using HFSS Software. The antenna resonates at a frequency of 3.5 GHz. The S11 parameter of the antenna is –40.2827 dB. The antenna has an impedance of 50.99 – j 0.15 Ohm. The impedance matching is excellent which satisfies the maximum power transfer theorem. Moreover, it has a maximum gain of 5.8263 dB and an efficiency of 88.40%. The VSWR value is 1.02, which is nearly ideal. Therefore, the reflection will be less and maximum signal transmission can take place. The CPA has a bandwidth of 200 MHz, within 3.4 GHz to 3.6 GHz which satisfies the TRAI standard. The simple structure, compact size, good radiation characteristics, proper impedance matching, and excellent gain make this CPA suitable for different 5G applications.

REFERENCES

[1] "Enabling 5G in India"– Telecom Regulatory Authority of India.

[2] D. Imran et al., "Millimeter wave microstrip patch antenna for 5G mobile communication," 2018 International Conference on Engineering and Emerging Technologies (ICEET), Lahore, 2018, pp. 1-6.

[3] A. Elfatimi, S. Bri, and A. Saadi, "Comparison between techniques feeding for simple rectangular, circular and triangular patch antenna at 2.45 GHz," 2018 4th International Conference on Optimization and Applications (ICOA), Mohammedia, 2018, pp. 1-5.

[4] S. Verma, L. Mahajan, R. Kumar, H. S. Saini, and N. Kumar, "A small microstrip patch antenna for future 5G applications," 2016 5th International Conference on Reliability, Infocom Technologies and Optimization (Trends and Future Directions) (ICRITO), Noida, 2016, pp. 460-463.

[5] R. Li, Q. Zhang, Y. Kuang, X. Chen, Z. Xiao, and J. Zhang, "Design of a Miniaturized Antenna Based on Split Ring Resonators for 5G Wireless Communications," 2019 Cross Strait Quad-Regional Radio Science and Wireless Technology Conference (CSQRWC), Taiyuan, China, 2019, pp. 1-4.

[6] W. S. T. Rowe and R. B. Waterhouse, "Investigation into the performance of proximity coupled stacked patches," IEEE Transactions on Antennas and Propagation, vol. 54, no. 6, pp. 1693-1698, June 2006.

[7] C. A. Balanis, Antenna Theory: Analysis and Design, 3rd Ed., John Wiley & Sons, 2005.

**Ninaad Patnaik**
**Aditya Ravi**
**Smarak Behera**
*Dept. of ECE*

# ALAN HARVEY GUTH

Alan Havey Guth, a native of New Jersey, is an American theoretical physicist and cosmologist. He discovered and developed the theory of cosmic inflation and he won the 2014 Kavli Prize for pioneering the theory of cosmic inflation.

Guth's first step to developing his theory of inflation occurred at Cornell in 1978. On the night of December 6, 1979 Alan Guth had the "spectacular realization" that would soon turn cosmology on its head. He imagined a mind-bogglingly brief event, at the very beginning of the big bang, during which the entire universe expanded exponentially, going from microscopic to cosmic size. That night was the birth of the concept of cosmic inflation. Such an explosive growth, supposedly fueled by a mysterious repulsive force, could solve in one stroke several of the problems that had plagued the young theory of the big bang.

Guth studied particle physics during the initial phase of his education but his interest toward cosmic dragged him to study physical cosmology. Alan Guth skipped his final year of high school to begin studies at the Massachusetts Institute of Technology in 1964. After his PhD in physics in 1971, he began a series of postdoctoral positions at Princeton, Columbia, and Cornell universities, and the Stanford Linear Accelerator Center. While at Cornell, he began collaborating with colleague Henry Tye on the creation of magnetic monopoles in the early universe, and it was this work which led to his proposal of an inflationary universe. Guth continues to work on inflation, including the possibility of igniting inflation in a hypothetical laboratory to create a new universe and whether inflation is eternal - it's always going on, somewhere in the universe.

Guth has been awarded the Franklin Medal for Physics, the Eddington Medal, the Isaac Newton Medal, the Dirac Prize, and the Gruber Prize in Cosmology, and has been elected to the U.S. National Academy of Sciences and the American Academy of Arts and Sciences.

As he once said in an interview-"The Big Bang theory says nothing about what banged, why it banged, or what happened before it banged", he dedicated himself towards explaining certain flaws of Big bang theory, the cosmic inflation, expanding of the universe etc. In his book "A Universe in your Backyard", he said-"It becomes very tempting to ask whether, in principle, it's possible to create a universe in the laboratory or a universe in your backyard by man-made processes". He also explained the number of useful purpose served by cosmic inflation to the world and his contributions are incomparable.

**Tanmaya Bal**
*7th SEM ,ECE-C*

# Blood Cell Counting using YOLO

***Abstract :*** *Blood cell count is an important test in medical diagnosis to evaluate overall health condition. Traditionally blood cells are counted manually using haemocytometer along with other laboratory equipment's and chemical compounds, which is a time-consuming and tedious task. In this work, the YOLO framework has been trained with a modified configuration BCCD Dataset of blood smear images to automatically identify and count red blood cells, white blood cells, and platelets. Overall the computer-aided system of detection and counting enables us to count blood cells from smear images in a few seconds, which is useful for practical applications.*

**Keywords:** Medical image processing, Blood image classification, , Blood cell count, Blood smear images, Blood cells detection, YOLO

## I. INTRODUCTION

With the development of machine learning techniques, image classification and object detection applications are becoming more robust and more accurate. As a result, machine learning based methods are being applied in different fields. Particularly, deep learning methods are being applied in different medical applications such as abnormality detection and localization in chest X-rays, automatic segmentation of the left ventricle in cardiac MRI, and detection of diabetic retinopathy in retinal fundus photographs. Thus, it is worth to look into deep learning based methods that can be applied to identify and count the blood cells in the smear images

Blood cell count is an important test often requested by medical professionals to evaluate health condition. Traditional manual blood cell counting system using haemocytometer is highly time consuming and erroneous and most of the cases accuracy vastly depends on the skills of a clinical laboratory analyst. Therefore, an automated process to count different blood cells from a smear image will greatly facilitate the entire counting process.

The main three types of cells that constitute blood are red blood cells (RBCs), white blood cells (WBCs), and platelets.[1, 2] RBCs also known as erythrocytes are the most common type of blood cell, which consists of 40–45% of blood cells. Platelets also known as thrombocytes are also in huge number in blood. WBCs also known as leukocytes are just 1% of total blood cells. RBCs carry oxygen to our body tissues and the amount of oxygen tissues receives is affected by the number of RBCs. WBCs fight against infections and platelets help with blood clotting. The count of these cells determines the ability of an organism to resist a particular infection and capability of the body system. The normal count of these cells is different for men, women, and children, etc. Low count of WBCs indicates the presence of infection while high count indicates an existence of infection, leukemia or tissue damage. An abnormal count of RBCs leads to anemia which results in mental tiredness, illness, weakness, dizziness. So the blood count helps to evaluate the health of person and detect the disorders.

## II. UNDERSTANDING YOLO

### A.YOLO

YOLO (You Only Look Once) is an object detection system which helps in determining the location of certain objects present in the image, as well as classifying those objects [3]. In this system a single convolutional network predicts the bounding boxes and the class probabilities for these boxes making it a faster object detection system. YOLO trains on full images and directly optimizes detection performance. This model has several benefits over traditional methods of object detection. YOLO is extremely fast. Because in this model simply a neural network runs on a new image at test time to predict detections. YOLO reasons globally about the image when making predictions. YOLO sees the entire image during training and testing and implicitly encodes contextual information about classes as well as their appearance. YOLO learns generalized representations of objects. When trained on natural images and tested on artwork, YOLO performs well compared to other detection methods.

### B.Working of YOLO

First, an image is taken and YOLO algorithm is applied. The image is divided into any number grids, depending on the complexity of the image [4]. Once the image

is divided, each grid undergoes classification and localization of the object. The objectness score of each grid is found. If there is no proper object found in the grid, then the objectness and bounding box value of the grid will be zero or if there found an object in the grid then the objectness will be 1 and the bounding box value will be its corresponding bounding values of the found object. Anchor

boxes are used to increase the accuracy of object detection. The working steps of YOLO is shown in fig.1.

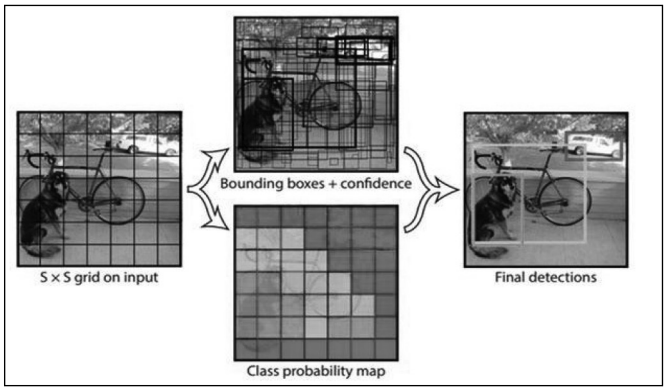


***Fig.1:*** *Working of YOLO*

**C. Grid Cells**

YOLO divides the input image into an S×S grid. Each grid cell predicts only one object [3]. For example, yellow grid cell predict the person object whose center falls inside the grid cell. Each grid cell predicts a fixed number of boundary boxes.

For each grid cell,

It predicts B boundary boxes and each box has one box confidence score.

It detects one object only regardless of the number of boxes B.

It predicts C conditional class probabilities (one per class for the likeliness of the object class).

**D. Boundary Box Prediction**

Each boundary box contains 5 elements: (x, y, w, h) and a box confidence score. x and y are offsets to the corresponding cell. w and h are the width and height of boundary box respectively[3]. The confidence score is how likely the box contains an object and how accurate is the boundary box. The conditional class probability is the probability that the detected object belongs to a particular class. If two or more grids contain the same object then the center point of the object is found and the grid which has that point is taken. For this, to get the accurate detection of the object two methods can be used and those are Intersection over Union (IoU) and Non-Max Suppression.

**E. Network Architecture**

YOLO v3 uses a variant of Darknet, which originally has 53 layer network trained on Imagenet. For the task of detection, 53 more layers are stacked onto it giving us a 106 layer fully convolutional layer underlying architecture for YOLO v3 [4]. Darknet-53 is the feature extractor and mainly composes of 3 × 3 and 1× 1 filters with skip connections like the residual network in ResNet. Darknet-53 has less BFLOP (billion floating point operations) than ResNet-152, but achieves the same classification accuracy at two times faster rate.

**F. Prediction at three scales**

Most classifiers assume output labels are mutually exclusive. It is true if the outputs are mutually exclusive object classes. For example, the output labels may be pedestrian and person which is not mutually exclusive[3]. Therefore, YOLO v3 uses independent logistic classifiers to calculate the likeliness of the input belongs to a specific label. YOLOv3 uses binary cross- entropy loss for each label to calculate the classification loss.

## III. DATASET

A publicly available dataset of annotated blood cell images called Blood Cell Count Dataset (BCCD) is used. It is a small-scale dataset for blood cells detection. The data set contains of roughly around 400 microscopic images of blood along with xml files containing the annotations and information about bounding boxes [4]. We have to identify and localize, in an image, whether a cell is RBC, WBC or Platelet. It has a total of 364 annotated smear images, but the dataset has some crucial flaw. After splitting the dataset into training (300) and testing (64) parts, it is found that one annotation file in the test set does not include any RBC, although the image contains RBCs. Moreover, three annotations file exhibit very low RBC than actual. So, we remove four fallacious files and the total size of the test set becomes 60. For the validation set, we randomly pick 60 training images with annotations.

## IV. IMPLEMENTATION AND RESULTS

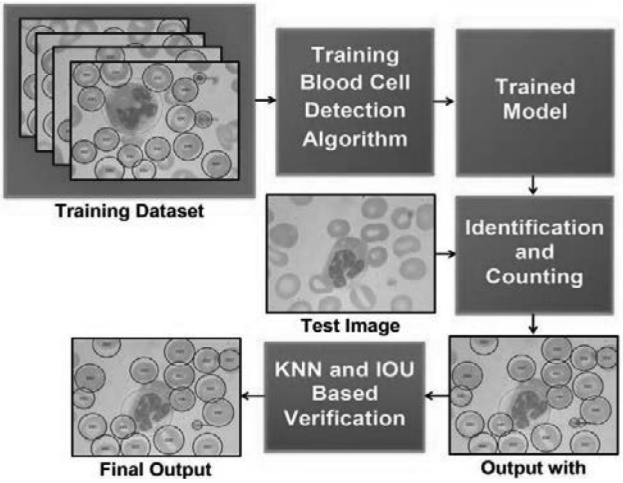


***Fig. 6.*** *VSWR characteristics of the proposed CPA*

Using deep learning object detection method the different types of blood cells are detected. Among the different object detection algorithms you only look once (YOLO) is chosen which gives faster and accurate results compared to other algorithms. The block diagram for blood cell identification and counting is shown in Fig. 2.

YOLO framework is trained to identify and count RBCs, WBCs, and platelets from blood smear images. The images are transformed into grayscale images and looking at the structures and features of the cells they are identified and further classified. To improve the counting accuracy, KNN algorithm is used. Then the trained model is tested with other images to observe the correctness of the method.

The original implementation of the Tiny YOLO configuration was trained for 20 different classes. To adopt it for blood cells identification, it is modified for three classes consisting of WBC, RBC, and platelets. Due to modifying the class number, the number of filters in the final convolutional layer in the CNN architecture is required to be changed as well. Of the 360 images of the dataset, 300 annotated blood smear images were used for training and 60 for testing [4]. During training, loss and moving average loss was recorded. Two different learning rates were used: 10-5 and 10-7. The weights were recorded and the model was evaluated. The weights are then used for testing purpose. We use our model to count the different cells in the validation dataset with different confidence threshold. For counting RBCs, confidence threshold is set to 0.55, for WBCs it is 0.35 and for platelets it is set to 0.25.

The test image is imported along with the trained weights. Blood Cells are predicted and counted. Our model is also used to detect and count blood cells from high- resolution blood cell smear images. These test images are of the size of 3872 x 2592 which is way higher than the size of our trained images of 640 x 480. So, to match the cell size of our trained images we divide those images into grid cells and run in each grid cell and then combine all the prediction results. In some cases platelets are counted twice. To improve counting accuracy of platelets, we use KNN algorithm in each platelet and determine its closest platelet and then using the intersection of union (IoU) between two platelets we calculate their extent of overlap. If the overlap is greater than ten percent, we ignore that cell to avoid the extra count.

YOLO framework is trained to identify and count RBCs, WBCs, and platelets from blood smear images. The images are transformed into grayscale images and looking at the structures and features of the cells they are identified and further classified. To improve the counting accuracy, KNN algorithm is used. Then the trained model is tested with other images to observe the correctness of the method.

The original implementation of the Tiny YOLO configuration was trained for 20 different classes. To adopt it for blood cells identification, it is modified for three classes consisting of WBC, RBC, and platelets. Due to modifying the class number, the number of filters in the final convolutional layer in the CNN architecture is required to be changed as well. Of the 360 images of the dataset, 300 annotated blood smear images were used for training and 60 for testing [4]. During training, loss and moving average loss was recorded. Two different learning rates were used: 10-5 and 10-7. The weights were recorded and the model was evaluated. The weights are then used for testing purpose. We use our model to count the different cells in the validation dataset with different confidence threshold. For counting RBCs, confidence threshold is set to 0.55, for WBCs it is 0.35 and for platelets it is set to 0.25.

The test image is imported along with the trained weights. Blood Cells are predicted and counted. Our model is also used to detect and count blood cells from high- resolution blood cell smear images. These test images are of the size of 3872 x 2592 which is way higher than the size of our trained images of 640 x 480. So, to match the cell size of our trained images we divide those images into grid cells and run in each grid cell and then combine all the prediction results. In some cases platelets are counted

twice. To improve counting accuracy of platelets, we use KNN algorithm in each platelet and determine its closest platelet and then using the intersection of union (IoU) between two platelets we calculate their extent of overlap. If the overlap is greater than ten percent, we ignore that cell to avoid the extra count.

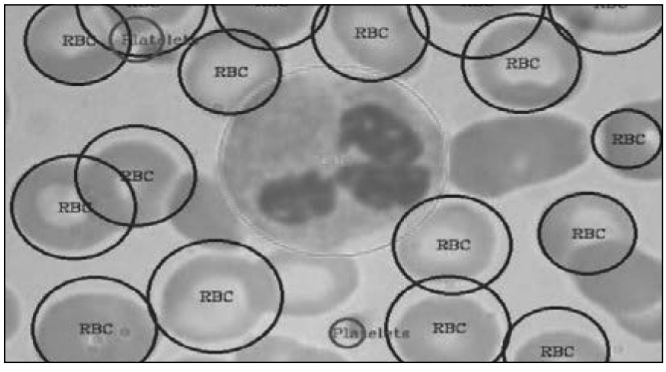


***Fig.1:*** *Working of YOLO*

The outputs of predictions on test image and classified output of HRI is shown in fig.3 and fig.4 respectively. The algorithm detected 17 RBC, 1 WBC and 2 Platelets.

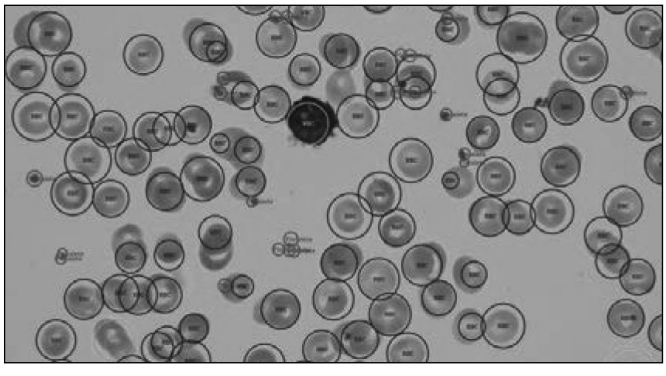

***Fig.1:*** *Working of YOLO*

## V. CONCLUSIONS

In this work, a machine learning approach to automatically identify and count blood cells from a smear image based on YOLO algorithm is presented. To improve accuracy, the method employed KNN and IOU based method to remove multiple counting of the same object. The proposed method is evaluated on publicly available datasets. It is observed for test dataset that, our method accurately identifies RBCs, WBCs, and Platelets with an accuracy of 96.09%, 86.89%, 96.36% manually. The proposed method has also been tested on a different dataset of higher resolution, where it has performed satisfactorily. With the accuracy and the detection performance of the proposed method, it can be said that, the method can ease up the manual blood cell identification and counting process.

## ACKNOWLEDGMENT

We would like to express our gratitude to our project guide, Mr. Nihar Ranjan Nayak, of CSE department for his guidance in carrying out this work.

## REFERENCES

1. Manish Chablani, YOLO-You only look once, real time object detection explained

2. N. Guo, L. Zeng, and Q. Wu, A method based on multispectral imaging technique for white blood cell segmentation, Computers in Biology and Medicine, vol. 37, no. 1, pp. 70–76, 2007.

3. N. Hazlyna and M. Y. Mashor, Segmentation technique for acute leukemia blood cells images using saturation component and moving l-mean clustering procedures, International Journal of Electrical, Electronic Engineering and Technology, vol. 1, pp. 23– 35, 2011.

4. P. R. Tabrizi, S. H. Rezatofighi, and M. J. Yazdanpanah, -Using PCA and LVQ neural network for automatic recognition of five types of white blood cells, in Proceedings of the 32nd Annual International Conference of the IEEE Engineering in Medicine and Biology Society (EMBC '10), pp. 5593–5596, September 2010.

**Neha Gupta, Swagata Upadhyay,**
**Arpita Panda, Sarthak Padhi**
*8th sem. CSE*

# CRISPR-Cas9 – Another step towards change!

Genome editing is a set of technologies that gives scientists the ability to shape an organism's DNA. This group of technologies has allowed genetic material to be attached, detached, or metamorphosed at particular locations in the gene sequence. Many approaches to genome editing have been developed over the years. The most recent one is known as "CRISPR-Cas9". It stands for: Clustered Regularly Interspaced Short Palindromic Repeats and CRISPR-associated protein 9. The CRISPR-Cas9 system has generated a lot of enthusiasm in the scientific community because it is swift, economical, precise and much greater in efficient than other existing genome editing methods.

The idea of CRISPR-Cas9 was cultivated from a naturally occurring genome editing system in bacteria called the "Escherichia Coli" (acronym being "E. coli"). The bacteria capture and mirror snippets of DNA (Deoxyribonucleic acid) from foreign micro-organisms like viruses, fungi, protozoans, etc., and use them to create DNA segments known as CRISPR arrays. The CRISPR arrays aid the bacteria to "recall" the viruses (or closely related ones). If the viruses try to infect again, then the bacteria produce RNA segments from the CRISPR arrays to target the viruses' DNA. The bacteria then use Cas9 or a similar enzyme to snip the DNA apart, which disables the virus. The CRISPR-Cas9 system has a similar mode of operation. Scientists create a small fragment of RNA (Ribonucleic acid) with a short "guide" sequence that latches to a specific target sequence of DNA in a genome. The RNA also binds to the Cas9 enzyme. As in bacteria, the modified RNA is used to recognize the DNA sequence, and the Cas9 enzyme attacks the DNA at the targeted location. Although Cas9 is the enzyme that is used most often, other enzymes like Cpf1 (Cas12a) and C2c2 (Cas13) can also be used. Once the DNA is cut, researchers use the cell's own DNA repair mechanism to attach or detach pieces of genetic material, or alter the DNA by replacing an existing segment with a customized DNA sequence.

Genome editing is one of the best possible methods for the prevention and treatment of deadly human diseases. Most research on genome editing is currently done to understand diseases using cells and animal models. The same methods of editing are also being performed on the dreaded "Corona Virus" and its mutations to learn the pattern and mutation cycle. Such a research gives an idea about the genome sequence in order to develop a safe and effective cure. Scientists are still in the process of determining whether this approach is safe and effective for use in people. It is being employed in research on a wide variety of diseases, including single-gene disorders such as cystic fibrosis, haemophilia, and sickle cell anaemia. It also holds promise for the treatment and prevention of more complex diseases, such as cancer, heart disease, mental illness, and human immunodeficiency virus (HIV) infection. There was a time when sequencing the human genome was a massive project at the cutting edge of science. Indeed, many thought it to be the pinnacle of biological research. Today, sequencing one's genome has never been cheaper, dropping from $95million to just $950 over the past ten years, CRISPR-Cas9 being the main reason behind it. With greater understanding of our genetics comes greater capacity for their manipulation. Gene editing currently stands as one of the most exciting areas within the biotech industry. Many of the proposed applications involve editing the genomes of somatic (non-reproductive) cells but there has been a lot of interest in and debate about the potential to edit germline (reproductive) cells as well. The main reason behind the debate being the changes made in germline cells that will be passed on from generation to generation. By contrast, the use of CRISPR-Cas9 and other gene editing technologies in somatic cells is uncontroversial. They have already been used to cure human disease on a small number of exceptional and/ or life-threatening cases.

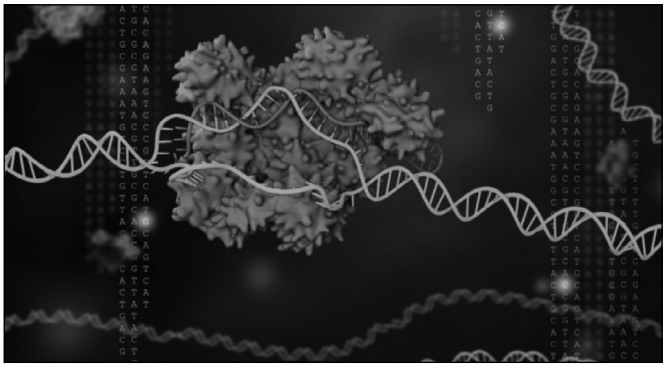

*CRISPR-Cas9 gene editing imaged for first time ( Courtesy: https://www.drugtargetreview.com/ news/46282/crispr-cas9-gene-editing-imaged-for-first-time/)*

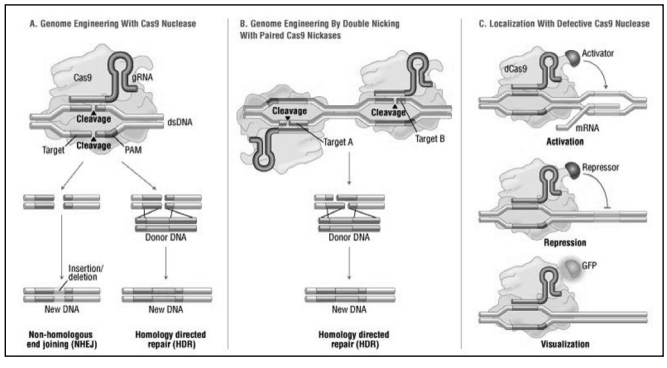


*Gene Editing Process by CRISPR_Cas9 (Courtesy: https://international.neb.com / tools-and-resources/feature-articles/crispr-cas9-and-targeted-genome-editing-a-new-era-in-molecular-biology)*

CRISPR-Cas9 is indeed one of the greatest breakthroughs in the world of biotechnology. Derived from the natural process of gene sequencing by E. coli, it sure has revolutionized the scientific world and will soon be administered routinely in humans. Many researches are still focusing on its use in animal and/or isolated human cells. Its main aim being to be used routinely used in order to treat human diseases. Though the system is still not completely accurate, work is being done till date in order to perfect this system of targeting a particular fragment and successfully operating it. When its all said and done, CASPR-Cas9 will surely become a step towards change, towards attaining a world free of several deadly diseases.

**Soumyakanta Panda**
*5Th sem. EEE*

## INNOVATIONS FOR COVID-19

**Indian company Techmax Solution designs toucheless elevator panels to fight COVID-19**

Thanks to this panel, called "Sparshless", no one needs to touch elevator buttons anymore. According to the company, it can work with all existing lifts, no modification is required. Instead of disinfecting the lift every day, this innovation could easily help stop the spread of the virus in apartments, hotels, malls, hospitals, offices and such public places.

**Japanese start-up Donut Robotics designs smart masks that connect to phones via Bluetooth**

The face mask, called 'C-Mask,' can be worn over regular, fabric-based masks. It connects to an app via Bluetooth, enabling it to transcribe speech to text messages, which are then sent via the user's smartphone. It can also translate from Japanese into eight other languages and amplify the user's voice, in case they are not heard through the mask.

**Microsoft launches digital skills initiative, making available its educational content, to help those hit by COVID-19**

Microsofts new global skills initiative aims at bringing more digital skills to 25 million people worldwide by the end of the year. Microsoft plans to combine existing and new resources from its LinkedIn and GitHub units (learning content, certifications, job-seeking tools), as well as from inside the rest of the company, and make them available for free or cheaply to those who are interested in up-skilling or retraining for new careers.

*New MIT robot using UV light to kill coronavirus could be used to disinfect warehouses, schools, and offices*

The system has already been used to sanitise the Greater Boston Food Bank. In tests, the robot covered a 4,000 square foot area of the warehouse within 30 minutes, providing enough light to neutralise around 90% of coronavirus particles. Tele-operators have first to teach the robot a route around the site, then it follows waypoints around a map of the venue. The next step is enabling the robot to adapt to changes in its environment.

*Source:*
https://www.covidinnovations.com/

# Increasing the Number of Fin and Studying its Impact on Various Parameters of the Fin-FET

***Abstract :*** *In this paper, we systematically examined the impact of inserting a second gate by hollowing out the fin, on the ac performance parameters including total gate capacitance(Cgg), RC delay (CggVDD/ION), cutoff frequency (fT), energy (E),Total power (PTotal), and leakage power (PLeakage) of hybrid FinFETs at the supply voltage, VDD with on-current ION. The RC delay, energy, and total power consumption are the primary factors limiting the operating frequency of the high-performance devices. Therefore, these electrical parameters are needed to be addressed in the architectural level of the fin based devices. In this paper, a calibrated numerical device simulation tool is used to achieve the best device performances of 50-nm hybrid FinFETs. From the simulated current–voltage (I–V) and capacitance–voltage (C–V) characteristics of hybrid FinFETs, the parameters Cgg, CggVDD/ION, fT, CV2, PTotal, and PLeakage are extracted to analyze the effect of the second gate inserted in the fin on the performance matrices of these devices. In addition, this paper proposes an optimum structural configuration for 50-nm hybridFinFET architecture for digital application perspective.*

## I. INTRODUCTION

A metal–oxide–semiconductor field-effect transistor is a field-effect transistor where the voltage determines the conductivity of the device. It is used for switching or amplifying signals. The ability to change conductivity with the amount of applied voltage can be used for amplifying or switching electronic signals. [1]

A MOSFET is by far the most common transistor in digital circuit, as hundreds of thousands or millions of them may be included in a memory chip or microprocessor. Since they can be included in a memory chip or microprocessor. And they can be made from either P-type or N-type semiconductors, complementary pairs of MOS transistors can be used to make switching circuits with very low power consumption, in the form of CMOS logic .MOSFETs are particularly useful in amplifiers due to their input impedance being nearly infinite which allows the amplifier to capture almost all the incoming signal. The main advantage is that it requires almost no input current to control the load current, when compared with bipolar transistors [2].

STRUCTURE OF MOSFET: It is a four-terminal device with source, gate, drain and body terminals. The body is frequently connected to the source terminal, reducing the terminals to three. It works by varying the width of a channel along which charge carriers flow (electrons or holes).The charge carriers enter the channel at source and exit via the drain. The width of the channel is controlled by the voltage on an electrode is called gate which is located between source and drain. It is insulated from the channel near an extremely thin layer of metal oxide. A metal-insulator-semiconductor field-effect transistor or MOSFET is a term almost synonymous with MOSFET between the drain and source, the current flows freely between the source and drain and the gate voltage controls the electrons in the channel. If we apply negative voltage, a hole channel will be formed [3].

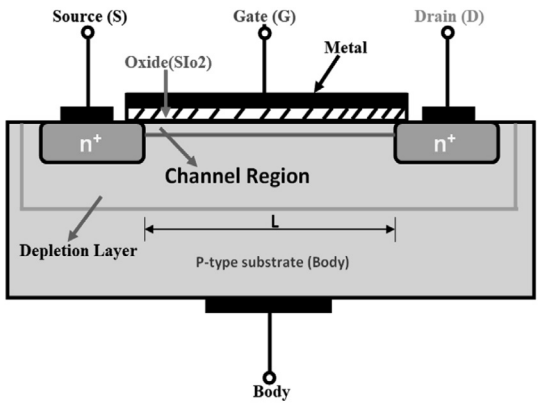


***Fig. 1.*** *Structure of the MOSFET*

A fin field-effect transistor (Fin-FET) is a multi gatedevice, a MOSFET (metal-oxide-s) shown in fig 1 is built on a substrate where the gate is placed on two, three, or four sides of the channel or wrapped around the channel, forming a double gate structure. Fin-FET is a type of non-planar transistor, or "3D" transistor as shown in fig.2. It is the basis for modern Nona electronics semiconductor device fabrication [2].

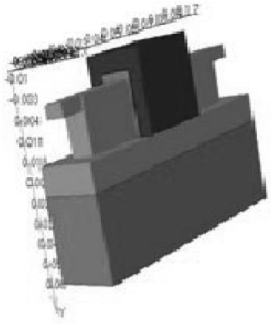

***Fig. 2*** *Structure of FINFET*

**ADVANTAGES OF FINFET OVER MOSFET:**

- Higher output current per input voltage.
- Higher switching speed and lower power consumption due to lower equivalent input capacitance and channel quantization effects.
- Better on/off contrast due to channel quantization effect.
- Channel quantization effect also reduce short-channel effects due to more effective physical separation of the source and drain regions.

**PARAMETERS OF FINFET**

The parameters on which the performance of the device will be verified upon are its analog parameters which are On-drain current(Ion)and OFF-drain current(Ioff), analog parameters helps us to know the optimum point at which the device should work as well as they give us better idea on the better usage of the device, the second parameter on which the device is checked are its linearity parameters, under linearity parameters comes the trans conductance and voltage intercept point, third comes the radio frequency parameters in it determines the frequency at which the device will work as well as it gives the cut-off frequency at which the device will produce normal output. The other parameters at which the impact of the two layer gate will depend are the energy, power and Rc-delay parameters for this the lower is the value the more efficient is the device These are the parameters on which the device will be judged upon and will be studied.

**I. DUAL FINFET**

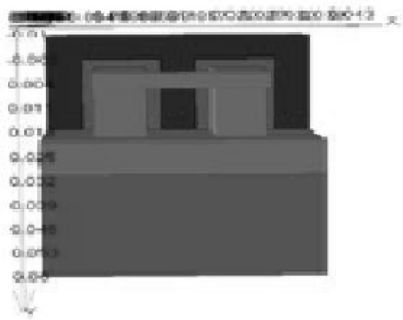

***Fig. 2*** *Structure of FINFET*

In basic finet, electrons are utilized only in the part of the substrate where the fin is acting. So, all the electrons can't be utilized. In order to utilize the amount of electrons to the fullest, we are applying this technique where we are using gate in between the two fins [3]. The structure of Finfet is shown in figure 3.

**II. TRIPLE FINFET**

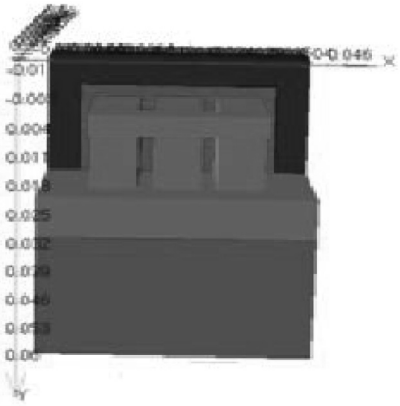

***Fig. 2*** *Structure of FINFET*

In basic fin, electrons are utilized only in the part of the substrate where the fin is acting. So, all the electrons can't be utilized. In order to utilize the amount of electrons to the fullest, we are applying this technique. But the difference from the above technique is that we are not applying a gate in between the fins.

**RESULTS ANALYSIS**

Here the important parameters like drain current, cutoff frequency, RC delay, energy and power are calculated of different structures.

**DRAIN CURRENT PLOT:**

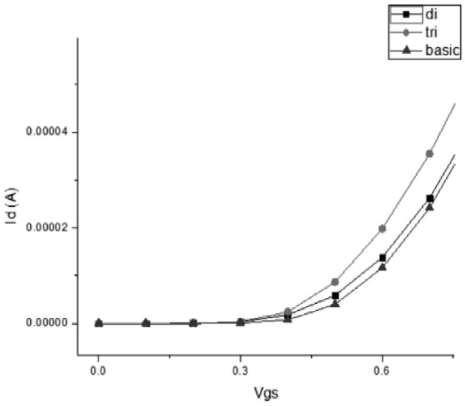


***Fig. 2*** *Structure of FINFET*

From the above figure 5 it is clear that the drain current for a constant voltage is increasing when the number of fin is increasing. That implies the tri-fin device provides more current compared to dual-fin and the dual fin device produces more current compared to basic finFET.

**FREQUENCY PLOT:**

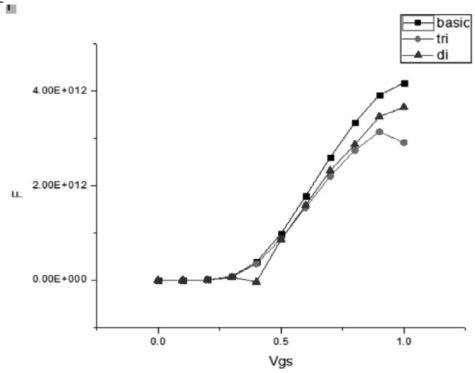


***Fig.6.*** *Comparison of frequency plot*

The cut-off frequency is found to be larger in case of basic finFET as shown in fig 6. The dual-fin having lesser frequency compared to that of basic. The tri-fin structure works for even lesser frequency.

**ENERGY PLOT:**

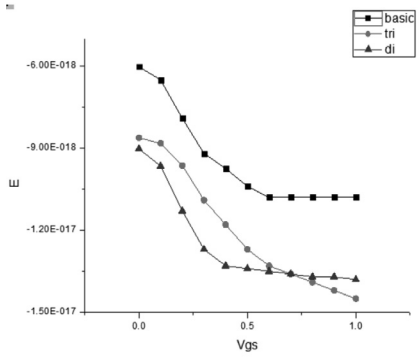


***Fig.7.*** *Comparison of energy plot*

The energy plot shown here in fig. 7 describes the energy consumed in the basic structure is more than the dual-fin and tri-fin structure.

**POWER PLOT:**

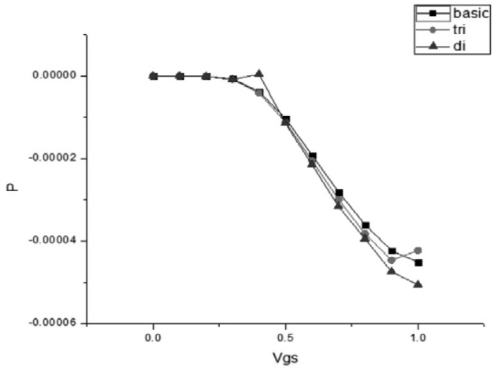


***Fig.8.*** *Comparison of power plot*

The power plot shown in fig. 8 here describes the power consumed in the basic structure is more than the dual-fin and tri-fin structure.

**RC-DELAY PLOT:**

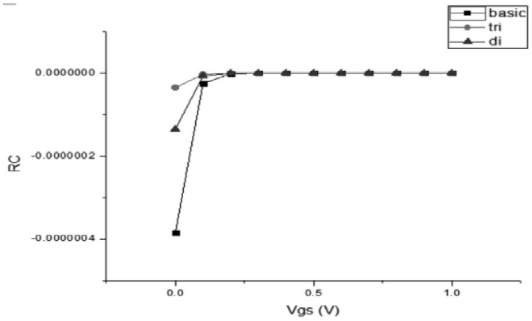


***Fig.9.*** *Comparison of RC-Delay plot*

The above comparison result shows that the RC delay in case of tri-fin material is less compared to dual-fin and basic finFET as shown in fig 9.

## CONCLUSIONS

We have successfully implemented two methodologies which are, first, we have two fins. Second, we have three fin. Out of the two methods that we implemented, the first method in which we have two fins showed the maximum current output as we are using a gate in between the two fins which help us to accumulate more electrons. Thus, helps in improvising the device parameters.

## REFERENCES

1. P. Elakkumanan , C. Thondapu , and R. Sridhar, "A gate leakage reduction strategy for sub-70 nm memory circuits," in IEEE Proceedings of the Workshop on Implementation of High Performance Circuits, 2004, pp. 145–148.

2. G. Prasad, "Novel low power 10T SRAM cell on 90nm CMOS," in 2nd International Conference on Advances in Electrical, Electronics, Information, Communication and Bio-Informatics (AEEICB), 2016. IEEE, 2016, pp. 109–114.

3. G. Razavipour ,A.Afzali-Kusha, and M.Pedram , "Design and analysis of two low-power SRAM cell structures," IEEE transactions on very large scale integration (VLSI) systems, vol. 17, no. 10, pp. 1551–1555, 2009.

**Siddhartha, Marmik Maharana, AbhijeetSahu, Manjeet Shekhar, Debraj Bhattacharjee, SamarpitaPattnaik, Chandana Dash, Jyoti Singh.**

*Dept. of AE & I*

# PERFORMANCE INVESTIGATION OF ADVANCED NANOSCALE DEVICES: AN ANALYTICAL MODELING AND SIMULATION STUDY

For the last few decades, MOSFETs are being continuously scaled down. As a result of this continuous scaling, several deleterious short-channel effects (SCEs) become prominent and start deteriorating the performance of traditional planar bulk MOSFETs. In order to reduce SCEs, various nonplanar multiple-gate device structures have been proposed in recent years to improve the electrostatic control of the channel by the gate terminal. Among them, Double Gate (DG), Surrounding gate (SRG) and FinFET technology based on Silicon-on-insulator (SOI) technology has been the forerunner of the CMOS technology in the last decade offering superior CMOS devices with higher speed, higher density, excellent radiation hardness and reduced second order effects for submicron VLSI applications. Recent experimental studies have invigorated interest in fully depleted (FD) SOI devices because of their potentially superior scalability relative to bulk silicon CMOS devices.

In this study, for the first time the effect of dimension scaling on different figure of merits for digital, analog and RF performance parameter such as drain induced barrier lowering (DIBL), subthreshold slope, threshold voltage roll-off, Transconductance, Transconductance Generation Factor, output Resistance, Intrinsic Gain, Cut-off Frequency, maximum Frequency of oscillation, Gain-Band-Width Product are need to be studied by developing simple computationally efficient physics-based analytical models and extensive simulation studies. Therefore, in this work, our main objective is to understand and analyze the design structure of novel nanoscale devices, exhibiting superior performance over traditional bulk MOSFETs in terms of device physics and scaling effects to become a competitive contender for usage in next generation system-on-chip applications and to provide incentive for further experimental exploration.

In this work, the remedies of prominent short-channel effects exhibited by deca-nanometer MOSFETs are studied by means of analytical modelling and the extensive numerical simulation studies. Unique features offered by different novel device structures such as InAs-based TFETs, gate-engineered MOSFETs and junctionless transistor structure have been studied to address the challenge of increasing short-channel effects and to show the efficacy to obtain improved analog/RF performance for deep-submicron VLSI integration.

**Dr Biswajit Baral**
*Dept. of ECE*

# Coal pollution linked to fatalities in India

IMF(International Monetary Fund) chief Christine Lagarde said pollution from coal generation plants causes about 70,000 premature deaths every year in India. According to her, environmental problems do not just end with climate change. Lagarde said she believes the world is facing economic, environmental and social crisis. “The planet is warming rapidly, with unknown and possibly dire consequences down the line. Across too many societies, the gap between the haves and have-nots is getting wider and strains are getting fiercer,” she said.

Stressing that climate change is clearly one of the great challenges of our time, Lagarde said it is a present reality for the world’s poorest and most vulnerable people. In India, the thermal power generation is 62.1% out of the total, of which 53.6% is from coal, whereas it is significantly less from Renewable Energy Sources (RES). Looking into the present environmental conditions RES should be given more priority than thermal sources, especially coal-based plants, with a vision that at least half of the country’s energy production should come from RES by the next decade.

**Publication Cell**
Tel: 99372 89499 / 8260333609
Email: publication@silicon.ac.in

www.silicon.ac.in

The Science & Technology Magazine

# Digital Digest

## Silicon Institute of Technology
सिलिकन प्रौद्योगिकी संस्थान



Bhubaneswar Campus
*An Autonomous Institute*
Silicon Hills, Patia
Bhubaneswar - 751024



Sambalpur Campus
*An Affiliated Institute*
Silicon West, Sason
Sambalpur - 768200

## Contents





**Make your submissions to:**
publication@silicon.ac.in